Biochem. J. (2011) **438**, 53–62 (Printed in Great Britain) doi:10.1042/BJ20110502

online data

A drug targeting only p110α can block phosphoinositide 3-kinase signalling and tumour growth in certain cell types

Stephen JAMIESON*†, Jack U. FLANAGAN*†, Sharada KOLEKAR‡, Christina BUCHANAN†‡, Jackie D. KENDALL*†, Woo-Jeong LEE‡, Gordon W. REWCASTLE*†, William A. DENNY*†, Ripudaman SINGH*, James DICKSON§, Bruce C. BAGULEY*† and Peter R. SHEPHERD†‡[1]

*Auckland Cancer Society Research Centre, Faculty of Medical and Health Sciences, University of Auckland, Private Bag 92019, Auckland 1042, New Zealand, †Maurice Wilkins Centre for Molecular Biodiscovery, University of Auckland, Private Bag 92019, Auckland, New Zealand, ‡Department of Molecular Medicine and Pathology, University of Auckland, Medical School, Private Bag 92019, Auckland 1042, New Zealand, and §School of Biological Science, University of Auckland, Private Bag 92019, Auckland 1042, New Zealand

Genetic alterations in PI3K (phosphoinositide 3-kinase) signalling are common in cancer and include deletions in PTEN (phosphatase and tensin homologue deleted on chromosome 10), amplifications of *PIK3CA* and mutations in two distinct regions of the *PIK3CA* gene. This suggests drugs targeting PI3K, and p110α in particular, might be useful in treating cancers. Broad-spectrum inhibition of PI3K is effective in preventing growth factor signalling and tumour growth, but suitable inhibitors of p110α have not been available to study the effects of inhibiting this isoform alone. In the present study we characterize a novel small molecule, A66, showing the *S*-enantiomer to be a highly specific and selective p110α inhibitor. Using molecular modelling and biochemical studies, we explain the basis of this selectivity. Using a panel of isoform-selective inhibitors, we show that insulin signalling to Akt/PKB (protein kinase B) is attenuated by the additive effects of inhibiting p110α/p110β/p110δ in all cell lines tested. However, inhibition of p110α alone was sufficient to block insulin signalling to Akt/PKB in certain cell lines. The responsive cell lines all harboured H1047R mutations in *PIK3CA* and have high levels of p110α and class-Ia PI3K activity. This may explain the increased sensitivity of these cells to p110α inhibitors. We assessed the activation of Akt/PKB and tumour growth in xenograft models and found that tumours derived from two of the responsive cell lines were also responsive to A66 *in vivo*. These results show that inhibition of p110α alone has the potential to block growth factor signalling and reduce growth in a subset of tumours.

Key words: p110α E545K mutation, pan-phosphoinositide 3-kinase (PI3K)/mammalian target of rapamycin (mTOR) inhibitor NVP-BEZ235; phosphoinositide 3-kinase α (PI3Kα), phosphoinositide 4-kinase (PI4K), *PIK3CA*, *PIK3CA* H1047R mutation.

INTRODUCTION

The three class-Ia PI3Ks (phosphoinositide 3-kinases; p110α/p110β/p110δ) and the sole class-Ib PI3K (p110γ) couple growth factor receptors and G-protein-coupled receptors to a wide range of downstream pathways [1–3]. These enzymes have different tissue distributions, difference in methods of activation and different kinetic properties [4–6], but they all use PtdIns(4,5)P_2 to produce PtdIns(3,4,5)P_3. The cellular levels of PtdIns(3,4,5)P_3 are tightly controlled by phosphatases, including PTEN (phosphatase and tensin homologue deleted on chromosome 10) which dephosphorylates PtdIns(3,4,5)P_3 back to PtdIns(4,5)P_2 [7,8]. The importance of this pathway in cancer is highlighted by the fact that defects in both the kinase and phosphatase activities are commonly observed in tumours. PTEN is a tumour suppressor gene whose function is commonly lost in tumours [7,8], whereas the *PIK3CA* gene, which codes for p110α, appears to be the most important form of PI3K involved in solid tumours as it is commonly mutated [9,10] or amplified [11] in such cancers. The mutations in *PIK3CA* mainly occur in two distinct regions of the gene. It is not fully understood how these mutations contribute to the development of tumours, but they do confer a modest increase in catalytic activity [12,13], are capable of inducing transformation of cultured cells [14–16] and are capable of inducing tumours *in vivo* [17,18]. However, evidence is emerging that the main two different hot spot mutations in *PIK3CA* represent functionally distinct oncogenic activities [12,13,19–23]. The full implications of *PIK3CA* gene amplification are not fully understood, but presumably act by increasing overall PI3K activity levels.

The identification of oncogenic mutations and amplifications in *PIK3CA* has spurred the development of a wide range of small-molecule inhibitors targeting PI3K, with many of these currently in clinical trials [2,24,25]. Most of the compounds developed to date target multiple PI3K isoforms and related kinases such as mTOR (mammalian target of rapamycin). Compounds in this class show efficacy in inhibiting growth of cells in culture and xenograft models [2,24,25]. However, a question that remains to be answered is whether selectively targeting p110α might achieve similar results given that this seems to be the predominant oncogenic form of class-I PI3Ks.

The potential importance of targeting p110α is shown by studies showing specific genetic knockdown of *PIK3CA* does block cell signalling and cell growth in a range of tumour lines [26–28]. To date the lack of suitable small-molecule inhibitors has meant that it has not been possible to properly evaluate whether pharmacological inhibition of p110α can achieve similar effects. Only one series of small molecules has been described

Abbreviations used: BID, twice daily dosing; ERK, extracellular-signal-regulated kinase; mTOR, mammalian target of rapamycin; PI3K, phosphoinositide 3-kinase; PI4K, phosphoinositide 4-kinase; PKB, protein kinase B; PTEN, phosphatase and tensin homologue deleted on chromosome 10; QD, once daily dosing; TGI, tumour growth inhibition.

[1] To whom correspondence should be addressed (email peter.shepherd@auckland.ac.nz).

Conflict of interest statement: P.R.S., W.A.D., J.D.K. and G.W.R. have consulted for and own stock in Pathway Therapeutics, a company developing PI3K inhibitors, although none of these compounds are used in the present study.

that has a high degree of selectivity for p110α compared with other PI3K isoforms [29]. One member of this family, PIK-75, has been used to study the role of p110α, but was found to have significant off-target activity [30], meaning it is difficult to know whether any actions of this drug are in fact due to its activity against PI3K. Despite these limitations, this drug has been used in some studies to infer that blocking p110α is sufficient to block signalling to Akt/PKB (protein kinase B) in some cell types but not others [28,31,32]. Furthermore, compounds related to PIK-75 have shown antitumour activity *in vivo*, hinting that p110α inhibition might be a useful therapeutic strategy [29,33]. However these findings cannot be confirmed until a suitably clean p110α-selective inhibitor is available.

In the present paper, we report the properties of A66, a compound that was recently found to be a potent p110α inhibitor [34]. We show that this compound is highly selective for p110α over other PI3Ks and has a high degree of specificity as it does not target other protein kinases tested. We use this to demonstrate that inhibition of p110α attenuates signalling in a subset of cell types that are characterized by having kinase domain mutations in *PIK3CA*, high p110α levels and high total class-1a PI3K activity. We go on to show that A66 has efficacy in retarding growth of tumours in *in vivo* xenograft models that use cell lines that were responsive in culture. These results show that inhibition of p110α alone has the potential to block growth factor signalling and reduce growth in a subset of tumours.

MATERIALS AND METHODS

Inhbitors

The *S*-enantiomer of A66 (Figure 1) was prepared as described in Patent WO 2009/080705 [35], except that 2-(tert-butyl)-4′-methyl-[4,5′-bithiazol]-2′-amine was converted into A66 in one-pot by addition of L-prolinamide directly to the intermediate imidazolide solution. Aqueous work-up followed by recrystallization from aqueous methanol gave A66 as a white solid with a 81 % yield. ^{1}H NMR (400 MHz, $CDCl_3$) δ 8.56 (br s, 1*H*), 7.03 (s, 1*H*), 6.76 (br s, 1*H*), 5.65 (br s, 1*H*), 4.62 (d, *J* 8.0 Hz, 1*H*), 3.62 (m, 1*H*), 3.49 (m, 1*H*), 2.52 (s, 3*H*), 2.43 (m, 1*H*), 2.03–2.20 (m, 3*H*), 1.45 (s, 9*H*). LC-MS (APCI$^+$) 394 (MH^+, 100 %). Analysis calculated for $C_{17}H_{23}N_5O_2S_2$: C, 51.89; H, 5.89: N, 17.80. Found C, 51.85; H, 5.84; N, 17.81. The *R*-enantiomer of A66 was synthesized in the same way, except that D-prolinamide was used. Compound SN34452 was prepared similarly using pyrrolidine. ^{1}H NMR (400 MHz, $CDCl_3$) δ 7.78 (br s, 1*H*), 7.02 (s, 1*H*), 3.48 (m, 4*H*), 2.54 (s, 3*H*), 2.00 (m, 4*H*), 1.45 (s, 9*H*). LC-MS (APCI$^+$) 351 (MH^+, 100 %). Analysis calculated for $C_{16}H_{22}N_4OS_2$: C, 54.83; H, 6.33; N, 15.98. Found C, 55.10; H, 6.47; N, 15.94.

NVP-BEZ-235 was synthesized as described previously [31]. PIK-75, TGX-221 and IC87114 were obtained from Symansis. LY294002 and wortmannin were obtained from Sigma–Aldrich.

Modelling

An energy-minimized model of A66 was generated using SKETCHER (SYBYL8.2, Tripos) and minimized using MAXMIN2 with the MMFF94s forcefield and MMFF94 charges. Minimization was performed using 1000 steps of step descents followed by conjugate gradients until convergence at the 0.05 kcal/(mol·A) level. A distance-dependent dielectric function was used with a dielectric constant of 80. The major tautomer at pH 7.4 was generated using ChemAxon software. Docking was performed using GOLDv5.0. The apo p110α structure (PDB code 2RD0) was prepared by stripping all water molecules and the addition of protons using SYBYL8.2, and side-chain orientations were modified according to the results of MolProbity [36]. The docking site was defined as an 18 Å (1 Å = 0.1 nm) cavity centred on the Ile^{800} CD1 atom. The Chemscore fitness function with kinase modification was used as the scoring function and 20 Genetic Algorithm runs were performed using a search efficiency of 200 % with all poses were kept. Atom types for both protein and ligand were generated automatically and all ligand flexibility terms were turned on, although Ring-NH_2 and Ring-NR1R2 were set to flip, other settings were kept at default. All docking poses were minimized and rescored using the kinase-modified Chemscore with receptor depth scaling implemented. X-ray crystal structures for p110γ (PDB code 2CHZ) and p110δ (PDB code 2WXR) were superimposed on to p110α using PyMOL (http://www.pymol.org) and docking was performed under the same conditions with the 18 Å cavity centred on the CD1 of Ile^{744} and Ile^{777} respectively.

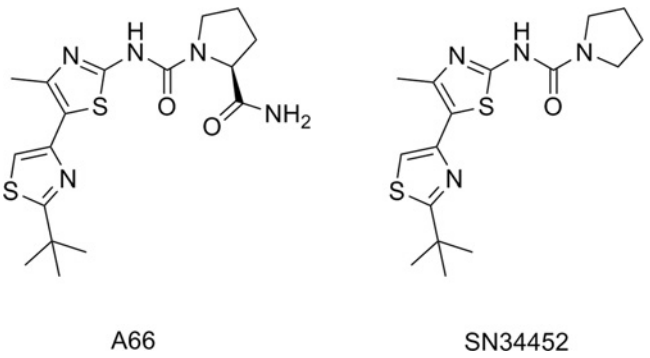

Figure 1 Structure of A66 and its inactive analogue SN34452

Assays

IC_{50} values were evaluated using the PI3K (human) HTRF Assay (Millipore, #33-016). p85α/p110δ was obtained from Invitrogen. All other isoforms were produced in-house by co-expressing full-length human p85α with the indicated human full-length catalytic subunit containing a histidine tag at the N-terminus to allow purification. The PI3Ks were titrated and used at a concentration between their EC_{65}–EC_{80} values. PI3K activity in immunoprecipitates was assayed as described previously [5] using an antibody to the N-SH2 (N-Src homology 2) domain of p85α (Symansis). Assays for other lipid kinases and protein kinases were performed by the National Centre for Protein Kinase Profiling (Dundee, U.K.) and Invitrogen Drug Discovery Services (Madison, WI, U.S.A.).

Pharmacokinetic methods

All animal experiments followed protocols approved by the Animal Ethics Committee of The University of Auckland. Age-matched specific pathogen-free male CD-1 mice were administered a single dose of A66 (10 mg/kg of body weight) in 20 % 2-hydroxypropyl-β-cyclodextrin in water or BEZ-235 in 15 % (v/v) DMSO, 20 % (v/v) 0.1 M HCl, 0.7 % Tween 20 and 64.3 % (v/v) saline. Mice were killed at five or six time points after dosing ($n = 3$/time point) and blood was removed by cardiac puncture into EDTA collection tubes (Becton Dickinson). Blood samples were centrifuged for 10 min at 6000 rev./min at 20 °C and the plasma supernatant was retained. Methanol was added to the plasma for protein extraction. Quantitative analysis was performed on an Agilent 6460 triple quadrupole LC-MS/MS (tandem MS) (Agilent Technologies) using multiple reaction monitoring

and electrospray ionization. For chromatographic separation, an Agilent Zorbax SB-C_{18} column (2.1 mm × 50 mm; 5 μm) was used with a mobile phase gradient of 20–100 % methanol in 0.1 % formic acid and 5 mM ammonium formate at a flow rate of 0.4 ml/min. Plasma drug concentrations were quantified against a calibration curve of known drug concentrations ranging from 10 to 10000 nM, with quality controls included at 65, 650 and 6500 nM. To prevent contamination from previous samples, a methanol slug was run between each plasma sample. Pharmacokinetic parameters were determined by noncompartmental analysis using WinNonlin 5.3 software (Pharsight).

Cell cultures and Western blotting

Treatment of cells with drugs and Western blotting was performed as described previously [31]. All antibodies for Western blotting were from Cell Signaling Technologies. Melanoma cell cultures were established and genotyped in-house. Established cell lines were obtained from A.T.C.C. and genotypes for cell lines were assigned on the basis of data from the COSMIC database (http://www.sanger.ac.uk/genetics/CGP/CellLines/).

Xenograft methods

Age-matched specific pathogen-free *Rag1*$^{-/-}$ or NIH-III mice were subcutaneously inoculated on the right flank with 5×10^6 U87MG, SK-OV-3 or HCT-116 cells in PBS. Tumour diameter as measured by electronic calipers was used to calculate tumour volume (mm^3) based on the formula $(L \times w^2) \times \pi/6$ (where L = longest tumour diameter and w = perpendicular diameter). A66 was administered in 20 % 2-hydroxypropyl-β-cyclodextrin (Sigma–Aldrich) in water, whereas BEZ-235 was administered in 10 % ethanol. Control mice were administered the A66 dosing vehicle alone. The drugs were dosed by intraperitoneal injection as the free base equivalent at a dosing volume of 10 ml/kg of body weight. For tumour pharmacodynamic studies, mice were administered a single dose of A66 or the control vehicle when tumours reached approximately 8–9 mm in diameter. Animals were killed 1 or 6 h after dosing and the tumours were removed, biopulverized and assayed for protein concentration (BCA protein assay; Sigma–Aldrich). For antitumour efficacy studies, dosing began when tumours were well established, averaging approximately 7 mm in diameter. Doses were administered once daily (QD) or twice daily (BID) with injections separated by a minimum of approximately 8 h. Different dosing schedules were used for the three xenograft models depending on the rate of tumour growth and the body weight tolerance of control mice. Animals were dosed daily for 21 days or twice daily for 16 days (SK-OV-3), daily for 14 days (U87MG) and daily for 7 days (HCT-116). Animals were monitored daily for any signs of emerging toxicity and body weight was recorded. Mice were killed if they developed moderate signs of toxicity or if body weight loss exceeded 20 % of starting weight. TGI (tumour growth inhibition) was calculated on the final day of dosing by determining the relative tumour size of drug-treated mice as a percentage of the average relative tumour size of control mice. The statistical significance of TGI values was determined by one-way ANOVA with Bonferroni multiple comparison analysis using GraphPad Prism 5.02.

RESULTS

Inhibitor specificity

We first characterized A66 and confirmed it was a potent inhibitor of the wild-type and oncogenic forms of p110α but not other class-I PI3K isoforms (Table 1). We found A66 has a much greater degree of selectivity for p110α than PIK-75. Given the important roles of class-II PI3Ks [37], class-III PI3K [38] and PI4Ks (phosphoinositide 4-kinases) [39] in growth factor signalling, we also assessed the activity of A66 towards these and found some limited cross-reactivity with the class-II PI3K PI3K-C2β and the PI4Kβ isoform of PI4K (Table 2). There was no inhibition of other lipid kinases or the related kinases DNA-PK and mTOR (Table 2). We also tested the inhibitory effects of 10 μM A66 effects on two large panels of 110 protein kinases (Supplementary Figure S1 at http://www.BiochemJ.org/bj/438/bj4380053add.htm) and 318 kinases (Supplementary Figure S2 at http://www.BiochemJ.org/bj/438/bj4380053add.htm). These show A66 is a very specific inhibitor of p110α, whereas PIK-75, the compound described previously as a p110α-selective inhibitor, inhibited a large number of protein kinases at this concentration (Supplementary Figure S1). Our data for TGX-221 and IC87114 generated using the HTRF assay agreed with previous studies using other assay methods and confirmed these are highly selective inhibitors of p110β and p110δ respectively (Table 1), although TGX-221 will cross-react with p110δ at higher concentrations [30,31,40]. We report further that these inhibitors do not have any major effects on a panel of 110 protein kinases (Supplementary Fig 1).

Table 1 IC_{50} for indicated drugs against different PI3K isoforms using HTRF assay

IC_{50} values are in nM. ND, not determined.

PI3K isoform	A66 *S*	A66 *R*	SN34452	PIK-75	TGX-221	IC87114
p110α	32	>5000	1560	6	>1000	>1000
p110α E545K	30	ND	540	24	>1000	>1000
p110α H1047R	43	ND	550	4.7	>1000	>1000
p110β	>12500	>12500	>25000	80	12	>1250
p110δ	>1250	>12500	>1000	164	130	41
p110γ	3480	ND	4350	33	>1250	>1250

Table 2 IC_{50} against PI3K-related kinases of A66 *S* form with or without the carboximide group

IC_{50} values are in nM. ND, not determined.

Kinase	A66 *S*	SN34452
PI3K-C2α	>5000	>10000
PI3K-C2β	462	6500
PI3K class-III	>5000	ND
mTOR	>5000	ND
DNA-PK	>5000	ND
PI4K α	>5000	>10000
PI4Kβ	236	478

A66 shares its central aminothiazole scaffold with the known PI3K inhibitor PIK-93, and the X-ray crystal structure of PIK-93 bound to the related p110γ isoform (PDB code 2CHZ) shows that the embedded hydrogen-bond donor acceptor group in this core interacts with the kinase domain through backbone amide and carbonyl groups of the inter-lobe linker region amino acid Val^{882} [30]. The aminothiazole unit in A66 may also influence its interaction with p110α by binding similarly, this is in part supported by the inhibition of PI4K by both these compounds [41]. The availability of the p110α X-ray crystal structure [42] allowed modelling of A66 in the p110α kinase domain and the likely mechanisms for its selectivity towards this compound were identified. The top-ranked binding mode for the A66

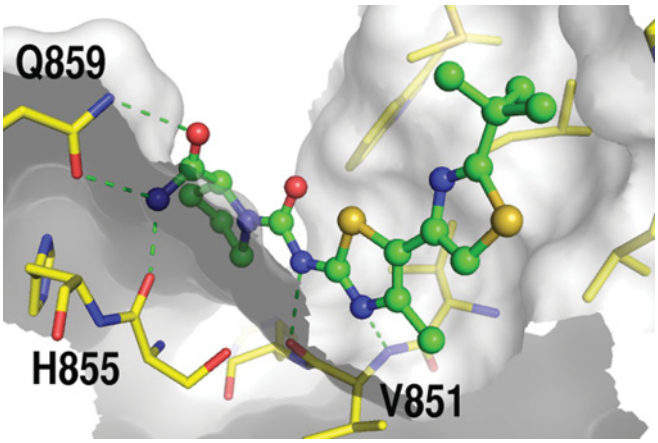

Figure 2 Model of A66 *S* form in binding pocket of p110α

S form docked into the p110α ATP-binding site (PDB code 2RD0), after minimization and rescoring with the kinase modified Chemscore scoring function using receptor depth scaling, is shown in Figure 2. Critically in this predicted binding mode, the ligand forms an interaction with Val^{851} of the inter-lobe linker region. Both the backbone amide and carbonyl of Val^{851} interact with the hydrogen bond donor and acceptor nitrogen atoms embedded in the central aminothiazole core, consistent with the binding mode observed for PIK-93 bound to p110γ [30]. The tertiary butyl-thiazole moiety extends from the amino-thioazole core into the lipophilic affinity pocket, whereas the pyrrolidine carboxamide group extends in the opposite direction towards a region of the binding site wall defined by the C-terminal lobe that contains p110α-specific residues, known to affect ligand binding [43]. In this predicted binding pose, the carboxamide amine moiety forms hydrogen bonds with the side-chain carbonyl group of Gln^{859} and possibly the backbone carbonyl group of Ser^{854} (Figure 2). Notably, the unminimized pose predicted a hydrogen bond interaction between both the carboxamide amide and carbonyl groups of the ligand and those in the Gln^{859} side chain. These residues were predicted previously to be involved in inhibitor interactions in the p110α active site [44].

We also investigated possible binding modes for the A66 *R* form, and observed that a pose similar to that of the S form was not found, and it failed to form a hydrogen bond interaction with the backbone amide of Val^{851} as well. In the top ranked pose, the *R* pyrrolidine carboxamide amino group was predicted to form a hydrogen bond with the Val^{851} backbone carbonyl. In this orientation, the ligand's central urea carbonyl was predicted to interact with the side-chain amino group of Gln^{859} and also the affinity pocket was not occupied. Interestingly, a few clashes between the protein and ligand were observed with the *S* form, whereas more were present for that of the *R* form. These results, taken together along with the higher Chemscore fitness value (*S*, 17.46 compared with *R*, 13.26), indicate that the A66 *S* form appears to complement better the p110α active site. In agreement with this, we find that the A66 *R* form lost inhibitory activity and did not inhibit p110α at 10 μM (Table 1).

Superimposition of the p110γ and p110δ kinase domains on to that of p110α illustrates that in p110γ Lys^{890} replaces the p110α Gln^{859}, whereas in p110δ Asn^{836} is the equivalent residue. As both these amino acid side-chains have hydrogen bond donor and acceptor groups that may interact with the ligand's pyrrolidine carboxamide, A66 was docked into the p110γ structure with the aminothiazole containing PIK-93 bound (PDB code 2CHZ) and the p110δ apo enzyme structure (PDB code 2WXR). The top ranked pose predicted for A66 binding to p110γ had a similar orientation to that predicted with p110α; however, the Chemscore fitness value was much lower, indicating a worse fit (Chemscore 7.29 compared with 17.46). An interaction with the p110γ Val^{882} backbone amide (the equivalent residue to p110α Val^{851}) was also not predicted, even though the PIK-93 aminothiazole forms this interaction. No interaction was observed with Lys^{890} and, moreover, the pyrrolidine group clashed with Trp^{812} on the N-terminal lobe wall of the active site, further supporting poor complementarity of this compound with p110γ. A low Chemscore value was also recorded for the top ranked pose in the p110δ active site (8.44 compared with 17.46), indicating a poor fit in this isoform. In the present study, no pose was found that was similar to those predicted in either the p110α apo structure or p110γ PIK93 structure, and an interaction with the backbone amide of the p110α Val^{851} equivalent, Val^{828}, was not observed. Neither was an interaction with Asn^{836}. The lack of similarity between the binding mode predicted for p110α and those for p110γ and p110δ suggest that other active site features, more than residue substitutions at Gln^{859}, may influence A66 binding. On the basis of the preferred binding model of A66 in p110α, we characterized the role of the carboxamide by docking an unsubstituted pyrrolidine derivative SN34552 (Figure 1). The binding mode was similar to that of A66, although the Chemscore was much lower in the absence of the predicted carboxamide-mediated hydrogen bonds (8.44 compared with 17.46), suggesting reduced potency. This was supported by biochemical data which showed that SN34452 has a much lower potency against p110α (Table 1) and clearly indicates that the pyrrolindine carboxamide group makes p110α-specific contacts that are accessible in both the wild-type and oncogenic forms. Interestingly, SN34452 largely retains its potency against PI4K TypeIIIβ (Table 2), which indicates the carboxamide is not critical for binding to this enzyme.

Effects of specifically inhibiting p110α on cell function

To investigate the role of p110α in regulating proximal elements of PI3K-dependent signalling pathways, we determined the ability of various concentrations of the A66 *S* form to acutely block the activation of Akt/PKB in a range of cell lines as assessed by both phosphorylation of Ser^{473} and Thr^{308} (Figure 3). Loading was controlled for by reprobing for total PKB (see Supplementary Figure S3 at http://www.BiochemJ.org/bj/438/bj4380053add.htm). We found that phosphorylation of both Ser^{473} and Thr^{308} is sensitive to LY294002 in all cell lines tested, implying that class-I PI3K activity is required for activation of Akt/PKB. However, we found the amount of the A66 *S* form required to inhibit phosphorylation of Ser^{473} and Thr^{308} followed two distinct patterns, being either sensitive to inhibition by the A66 *S* form at concentrations consistent with it acting through p110α or being resistant. The most obvious feature of the sensitive cell lines was that they harboured H1047R mutations in *PIK3CA*, whereas all other cell lines were resistant. As a control we tested the effect of the A66 *R* form and found it was not able to inhibit the phosphorylation of Akt/PKB (see Supplementary Figure S4 at http://www.BiochemJ.org/bj/438/bj4380053add.htm).

We then went on to investigate this in more detail in a larger panel of cell lines. The broader panel included early passage melanoma cultures that were genotyped in-house (NZM lines) [45]. The latter are likely to have characteristics more representative of real tumour tissue. In these studies we used PIK-75 as an alternative p110α inhibitor and we found that a low concentration of PIK-75 also blocks the insulin-stimulated

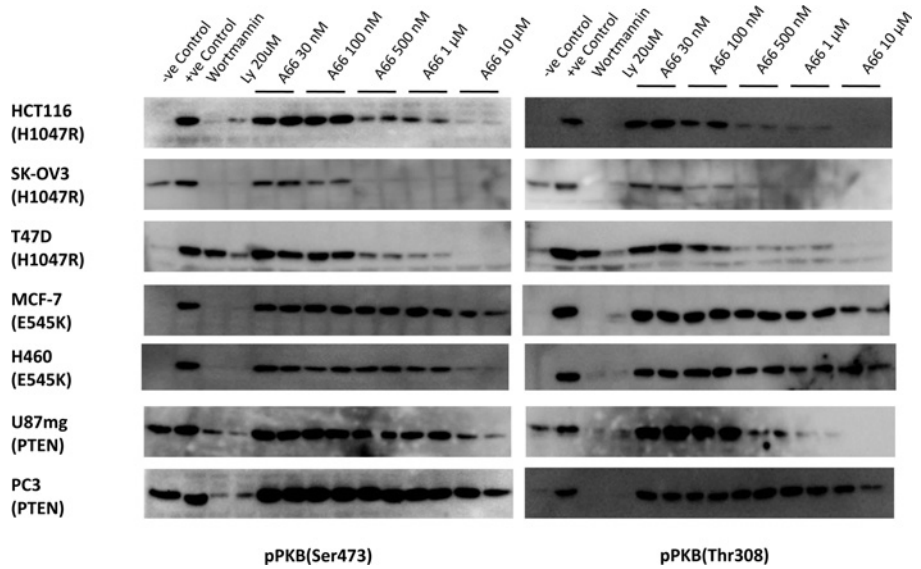

Figure 3 Effect of A66 *S* form on activation of Akt/PKB in cell lines

The indicated cell lines were serum-starved overnight and then treated with the indicated concentration of drug or DMSO vehicle for 15 min prior to stimulation with 500 nM insulin for 5 min. Cells were lysed and then analysed by Western blotting with the indicated antibody. Ly, LY294002.

phosphorylation of Thr^{308} and Ser^{473} on Akt/PKB in all lines harbouring *PIK3CA* H1047R mutations (Figure 4A). TGX-221 and IC87114 had no effect in these cells.

PIK-75 was less effective in cell lines that lack the H1047R mutation (Figure 4B), with the main exception being MCF7 cells, where both PIK-75 and TGX-221 had a partial inhibitory effect. In other cells, the activation of Akt/PKB was not inhibited by TGX-221 or IC87114 at concentrations at which they would be specifically inhibiting p110β or p110δ respectively. However, in these cells, the combination of PIK-75, TGX-221 and IC87114 together did block activation of Akt/PKB, which was consistent with the finding that wortmannin and LY294002 were also effective.

To further understand why certain cell lines are sensitive to p110α inhibitors, we compared total levels of class-Ia PI3K activity in the eight cell lines used in Figure 3. The cell lines that were responsive to the p110α inhibitors have significantly higher total levels of PI3K (Figures 5A and 5B). We next compared total levels of p110α and p110β protein in the cell lines used (Figure 5C). The levels of p110α were highest in the cell lines that were responsive to A66 and PIK-75. These cells also had levels of p110β that were higher than the other cell lines, with the exception of MCF7 cells which also had high levels of p110β. It is of note that the MCF7 cells were the only cell line that had a partial response to TGX-221 (Figure 4B) and this may relate to the ratio of p110β/p110α in these cells.

Demonstrating A66 is effective *in vivo*

To investigate whether the inhibitory effects of A66 *S* on activation of Akt/PKB signalling translated into the ability to block cell growth *in vivo*, we performed xenograft studies alongside the well-established pan-PI3K inhibitor BEZ-235 in U87MG cells, which are PTEN-null, and HCT-116 and SK-OV-3 cells, both of which contain H1047R mutations. First, we determined the optimal dosing strategy for xenograft studies by investigating the drug pharmacokinetics after a dose of 10 mg/kg of body weight by intraperitoneal injection in CD-1 mice. Despite a short half-life of only 0.42 h, the large C_{max} (8247 nM) of A66 *S* that was reached 30 min after dosing ensured that the $AUC_{0\text{-inf}}$ (area under the curve from zero time to infinity) (6809 nM·h) was similar to that of BEZ-235 (7333 nM·h), which has a longer half-life of 2.73 h (Table 3). Furthermore, we tested the effect of the A66 *S* form on SK-OV-3 tumour tissue *in vivo* using a single dose of 100 mg/kg of body weight to determine whether a long-lasting effect of the drug could be achieved on target tissues (Figure 6). These studies show that A66 *S* causes a profound reduction in the phosphorylation of Akt/PKB and p70 S6 kinase, but not of ERK (extracellular-signal-regulated kinase), at both 1 and 6 h after dosing (Figure 6). This is consistent with A66 *S* having a full inhibitory effect on PI3K signalling in the tumours during this time. In the present study, levels of A66 *S* in plasma were determined to be 21.1 ± 1.2 μM and 9.1 ± 1.1 μM at 1 and 6 h after drug injection, whereas levels of A66 *S* in the tumour were 22.7 ± 2.1 μM and 16.0 ± 1.3 μM at the same time points. Thus, the retention of drug in the tumour is likely to explain the persistence of the inhibitory effect.

On the basis of the pharmacokinetic and pharmacodynamic findings, A66 *S* was dosed QD at 100 mg/kg of body weight for up to 21 days or BID at 75 mg/kg of body weight for 16 days in tumour efficacy studies. Both dosing strategies induced a significant delay in growth of SK-OV-3 xenografted tumours, which was even greater than that induced by the well-established pan-PI3K inhibitor BEZ-235 (Figure 7A). At the final day of dosing, the average TGI for A66 *S* form was 45.9 % of control (QD; $P < 0.05$) and 29.9 % of control (BID; $P < 0.01$) (Table 4). QD A66 *S* was well tolerated in this xenograft model with minimum body weight loss; however BID treatment was associated with moderate body weight loss and two deaths, although it is not clear whether the deaths were due to drug toxicity or other causes since these mice did not show significant body weight loss (Figure 7B). In comparison, BEZ-235 induced a non-significant reduction in tumour growth and was even less tolerated, with moderate body weight loss and four deaths. QD dosing of A66 *S* in an HCT-116 xenograft model also induced a significant reduction in tumour volume with a TGI of 77.2 % of control ($P < 0.01$) at the end of dosing, but caused a non-significant reduction in tumour volume in the U87MG xenograft model (Table 4 and Supplementary Figure S5

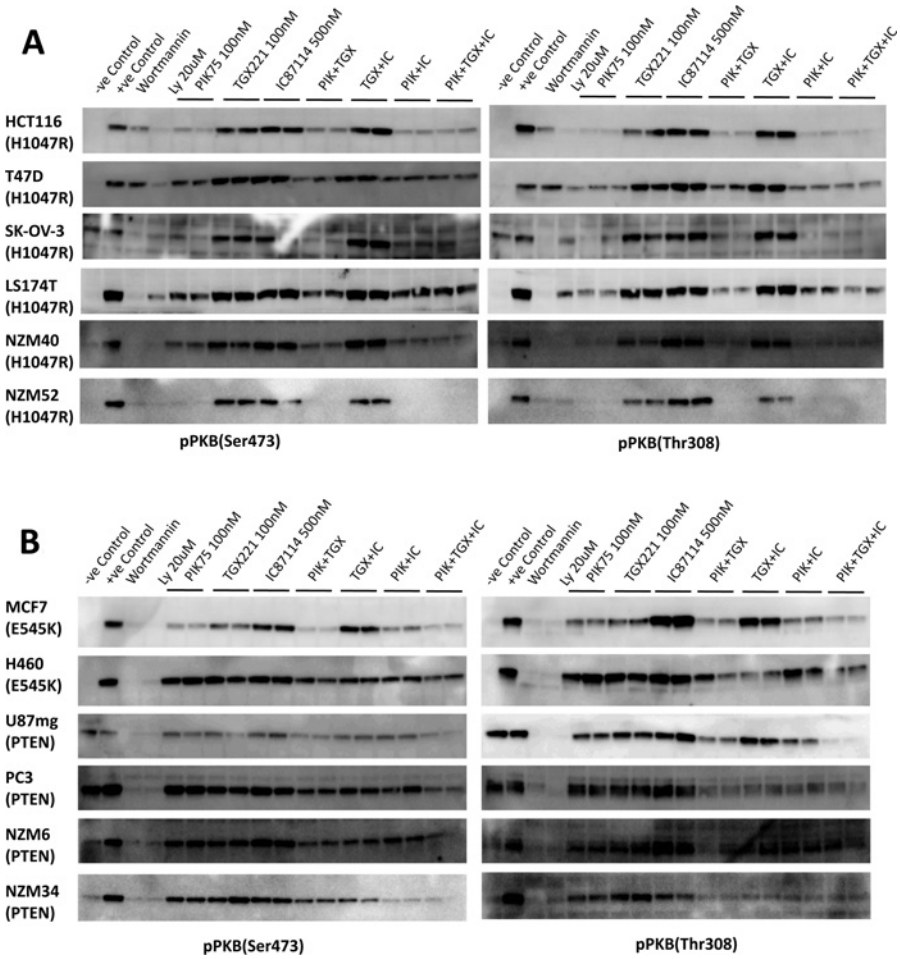

Figure 4 Effect of isoform-selective inhibitors of PI3K on activation of Akt/PKB

The indicated cell lines harbouring H1047R mutations (**A**) or harbouring other mutations (**B**), were serum-starved overnight and then treated with the indicated concentration of drug or DMSO vehicle for 15 min prior to stimulation with 500 nM insulin for 5 min. Cells were lysed and then separated by SDS/PAGE using 20 μg of protein per lane for all cell types, except T47D, SK-OV-3 and MCF7. Western blots were performed with the antibodies indicated. LY, LY294002; PIK, PIK-75.

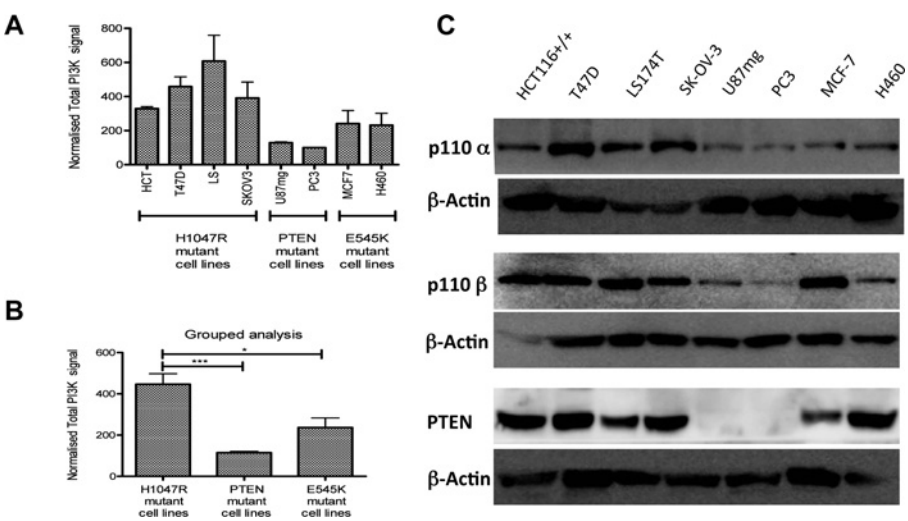

Figure 5 Levels of PI3K activity in different cell lines

(**A**) To assess the relative levels of PI3K activity in different cell lines, PI3K activity was measured in p85 immunoprecipitates from equivalent amounts of cell lysate. Results for the indicated cell lines were normalized to those for PC3 cells and are shown as means $\pm$ S.E.M. ($n = 4$ for each). (**B**) The combined results for all cells of the same genotype. Statistical analysis was performed using grouped ANOVA (*$P < 0.05$, ***$P < 0.005$). (**C**) Equal amounts of the indicated cell lysates were analysed by Western blotting for p110α, p110β and PTEN and reprobed to test for even loading with β-actin.

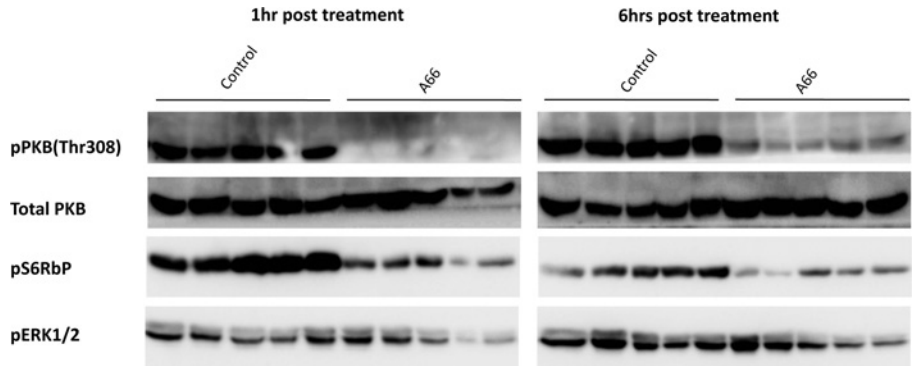

Figure 6 Effect of A66 *S* form on PI3K signalling in SK-OV-3 tumours

Western blotting was used to determine the phosphorylation status of Akt/PKB, p70 S6 kinase (pS6RbP) and ERK in SK-OV-3 tumours from mice 1 and 6 h after a single dose of A66 (100 mg/kg of body weight) or the control vehicle ($n = 5$).

Table 3 Plasma pharmacokinetic properties of A66 *S* form and BEZ-235 in mice after a single intraperitoneal dose of 10 mg/kg of body weight

Drug	C_{max} (nM)	T_{max} (h)	$AUC_{0\text{-}inf}$ (nM · h)	$T_{1/2}$ (h)
A66	8247	0.5	6809	0.42
BEZ-235	1863	0.25	7333	2.73

at http://www.BiochemJ.org/bj/438/bj4380053add.htm). In contrast, BEZ-235 significantly reduced U87MG tumour growth (TGI = 61.1 % of control; $P < 0.05$), but had no effect on HCT-116 tumours. The drugs were well tolerated in both the U87MG model, despite the toxicity with the same dose level of BEZ-235 in the SK-OV-3 study, and in the HCT-116 model, where a lower dose (10 mg/kg of body weight) of BEZ-235 was used due to the moderate body weight loss of control-treated mice.

DISCUSSION

The present study demonstrates that A66 *S* is a highly specific and selective inhibitor of p110α that is suitable for *in vitro* and *in vivo* studies. The contacts made by the carboxamide group give A66 *S* its potency and selectivity for p110α but, interestingly, it does inhibit PI4K IIIβ at concentrations approximately one order of magnitude higher. This is not surprising given the degree of homology between these enzymes in the catalytic sites [41]. However, SN34452 retains this activity against PI4K IIIβ when the carboxamide is removed (Table 2), which makes this one of the more selective PI4K IIIβ inhibitors described to date [41]. The other is PIK-93, which is structurally quite different from A66 apart from sharing an amino thiazole core, but it also inhibits both p110α and PI4K IIIβ, again highlighting the similarities in the catalytic site of these two enzymes [41].

Our results confirm previous studies that highlight the limitations of using PIK-75 and related compounds [30]. However, PIK-75 can still play a useful role as a backup for confirmatory experiments and it is worth noting that PIK-75 complements A66 in that it does not inhibit the two non-p110α lipid kinases that A66 targets, i.e. PI4K IIIβ and PI3K-C2β. Our studies also add extra weight to the case for TGX-221 and IC87114 being considered as highly selective inhibitors of p110β and p110δ if used at suitable concentrations.

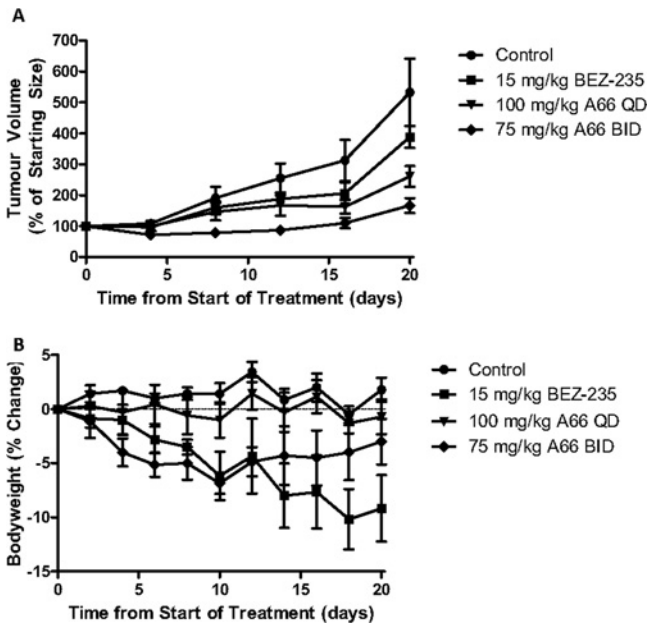

Figure 7 *In vivo* antitumour efficacy and body weight change following treatment with A66 *S* form and BEZ-235 in a SK-OV-3 tumour xenograft model

A66 was administered QD × 21 at 100 mg/kg of body weight or BID until day 16 at 75 mg/kg of body weight, and BEZ-235 was administered QD × 21 at 15 mg/kg of body weight. (**A**) Relative mean tumour volume following treatment with A66 and BEZ-235. Using one-way ANOVA analysis, the significance of tumour shrinkage compared with controls was calculated at days 8,12, 16 and 20 and found to be significantly different in the following conditions; BID A66 day 8 ($P < 0.05$), BID A66 day 12 ($P < 0.005$), BID A66 day 12 ($P < 0.005$), BID A66 day 16 ($P < 0.005$), BID A66 day 20 ($P < 0.01$), QD A66 day 16 ($P < 0.05$) and QD A66 day 20 ($P < 0.05$). (**B**) Bod yweight change from start of treatment in mice treated with A66 and BEZ-235. Values are means ± S.E.M. for seven or eight mice per group.

The finding that A66 *S* potently blocks phosphorylation of Akt/PKB in a subgroup of the cell lines tested demonstrates that some cell types are highly dependent on p110α activity. This is consistent with genetic studies which show that knockdown of p110α blocked signalling to Akt/PKB in cell lines harbouring mutations in PI3K [26,27]. It also supports previous studies using PIK-75 [28,31,33] and A66 [34] and suggests at least some cell types are more sensitive to p110α inhibitors. The finding that TGX-221 and IC87114 alone do not inhibit the phosphorylation of Akt/PKB at Ser^{473} or Thr^{308} in any of the cell lines tested,

Table 4 Summary of TGI and toxicity parameters for BEZ-235 and A66 *S* form in the SK-OV-3, HCT-116 and U87MG xenograft models

BWL, body weight loss; NS, not significant.

Xenagraft model		Control	BEZ-235	A66
SK-OV-3	Dose (mg/kg of body weight)	–	15	100
	Schedule	QD × 21	QD × 21	QD × 21
	BWL nadir (%)	− 2.0 ± 1.9	− 9.5 ± 6.6	− 4.3 ± 2.2
	Number of deaths/*n*	0/7	4/7	0/7
	TGI (%) (day 20)	–	69.4 ± 6.4	45.9 ± 4.6
	P value		NS	<0.05
HCT-116	Dose (mg/kg of body weight)	–	10	100
	Schedule	QD × 7	QD × 7	QD × 7
	BWL nadir (%)	− 6.7 ± 2.9	− 5.9 ± 1.8	− 6.0 ± 2.0
	Number of deaths/*n*	0/7	0/7	0/7
	TGI (%) (day 7)	–	117.7 ± 6.6	77.2 ± 2.7
	P value		NS	<0.01
U87MG	Dose (mg/kg of body weight)	–	15	100
	Schedule	QD × 14	QD × 14	QD × 14
	BWL nadir (%)	− 5.5 ± 3.0	− 8.4 ± 5.4	− 8.7 ± 3.1
	Number of deaths/*n*	0/7	0/5	0/5
	TGI (%) (day 11)	–	61.1 ± 8.1	78.0 ± 9.4
	P value		<0.05	NS

with the exception of a partial effect of TGX-221 in MCF7 cells, indicates that this pathway is not reliant on the catalytic activities of p110β and p110δ in most cells. The findings with regard to p110δ are not unexpected, but the findings with TGX-221 are somewhat at odds with some previous studies. Although no oncogenic mutations have been found in p110β, overexpression of p110β is capable of inducing transformation [46]. Knockdown of *PIK3CB* has been shown to block the ability of PTEN-deficient cell lines to form foci in *in vitro* transformation assays [26,47,48] and in *in vivo* tumour models. The knockdown of *PIK3CB* has also been reported to result in a small reduction in Akt/PKB phosphorylation in PTEN-deficient cells [26,47,48]. Although some functions of p110β appear to be independent of its lipid kinase activity [49], the finding that TGX-221 blocks signalling to Akt/PKB in PTEN-deficient cells has been taken as evidence that the catalytic activity of p110β is required in this context [47,50]. However, it should be pointed out that those studies used a 20- to 100-fold higher concentration of TGX-221 than those used in the present study, which would provide for a significant opportunity for cross-reactivity with other PI3K isoforms. In support of this, Wee et al. [26] found that 2 μM TGX-221 was required to induce reduction in Akt/PKB activation in PTEN-deficient cell lines, but that at these concentrations also partially reduced activation of Akt/PKB in the DLD1 cell line that harbours a *PIK3CA* mutation. This would be consistent with our results from the present study which demonstrate that binary combinations of A66 *S*, TGX-221 and IC87114 induce varying degrees of partial inhibition of activation of Akt/PKB, whereas the combination of all three drugs induced maximal inhibition. This indicates that the three class-Ia PI3K isoforms are functionally redundant to some extent and can substitute each other in signalling to Akt/PKB in these PTEN-null cells, as has been observed previously in other cell types [31,51,52].

In the present study, activation of Akt/PKB was sensitive to p110α inhibitors in H1047R cells but not in PTEN-null cell lines and those harbouring E545K mutations, which is in agreement with the studies of Torbett et al. [32] who used PIK-75. It would be tempting to conclude that the sensitivity to p110α inhibitors is a direct consequence of the presence of the H1047R mutation, since this isoform has increased catalytic activity [13]. However, the *PIK3CA* mutants are not intrinsically sensitive to A66 or PIK-75 (Table 1), and gene knockout studies have shown that sensitivity of HCT-116 cells to p110α-selective PIK-75 analogues is not changed by deletion of the H1047R allele of *PIK3CA* [33]. Furthermore, the study by Torbett et al. [32] showed that MCF10A cells and Hs578t cells were also sensitive to PIK-75. The latter can be explained by the fact that this line was subsequently found to have a mutation in *PIK3R1* (Cosmic database) and such mutations have been shown to be sensitive to p110α inhibitors [34]. Although MCF10A cells have no reported mutations in PI3K signalling pathways, a certain sub-population of these cells has been reported to have high PI3K activity [53]. This is consistent with another study which observed PI3K is not mutated in medulloblastoma, but that p110α is overexpressed and that such cells are very sensitive to PIK-75 [22]. Furthermore, we have observed previously in other cells that the degree of PIK-75 sensitivity is proportional to the relative amount of the total PI3K activity that is attributable to p110α [31]. Our results from the present study also show that the cells with high overall class-Ia PI3K and p110α protein levels are the ones that are sensitive to p110α inhibitors. Therefore the increased catalytic activity of the H1047 mutant may not be sufficient on its own to confer sensitivity to p110α inhibitors, but rather it may be the total levels of p110α (mutant or wild-type) in the cells that is most important. In this regard it is worth noting that evidence has recently been presented to indicate that at least part of the effect of the H1047R mutant might be to stabilize p110α levels in the cell [53]. The relative levels of class-Ia PI3K isoforms is also likely to be important and it is in this regard it is noteworthy that MCF7 cells are partially responsive to TGX-221, suggesting a dependence on p110β, and this cell line is the only one where we found high p110β and low p110α levels. Further studies will be required to clarify these issues.

The reason for the difference in characteristics between the H1047R and E545K cell lines is not clear. However, a number of studies have indicated that these two main oncogenic forms of p110α are likely to function differently *in vitro* and *in vivo* [12,13,19–23]. In particular, the helical domain mutants appear to signal independently of the p85 adapter subunit, and hence of activation by receptor tyrosine kinases, but require Ras [54]. The kinase domain mutants, on the other hand, require p85 but are independent of Ras [54]. Again it will require further studies to clarify this issue.

The finding that A66 *S* is more effective at inducing growth delay in the HCT-116 and SK-OV-3 xenograft models than the pan-PI3K/mTOR inhibitor BEZ-235 [55] demonstrates that a p110α-selective inhibitor can be effective at slowing cell growth in the absence of mTOR inhibition in certain cell types. In addition, although A66 *S* did not induce tumour regression in xenograft models, the ability to induce growth delay indicates p110α-selective inhibitors have to ability to be effective as cytostatic agents in some tumour types. Further studies will be required to determine whether A66 might contribute to tumour regression as part of a combination drug treatment strategy.

AUTHOR CONTRIBUTION

Stephen Jamieson, Jack Flanagan, Bruce Baguley and Peter Shepherd developed concepts, and designed and supervised experiments. Jackie Kendall, Gordon Rewcastle and William Denny designed and performed the chemical synthesis. Stephen Jamieson, Jack Flanagan, Sharada Kolekar, Christina Buchanan, Jackie Kendall, Woo-Jeong Lee, Gordon Rewcastle, Ripudaman Singh and James Dickson performed experiments. Peter Shepherd, Jack Flanagan, Gordon Rewcastle and Stephen Jamieson were the main contributors in the writing of the paper. Sharada Kolekar, Christina Buchanan and William Denny made minor contributions in the writing of the paper.

ACKNOWLEDGEMENTS

We thank Aaron Thompson and Phil Kestell for their help with tumour xenograft and pharmacokinetic studies, and Dr Graham Atwell for synthesizing the A66 *R* form.

FUNDING

This work was funded by the Health Research Council of New Zealand [grant number 09-388], the Maurice Wilkins Centre for Molecular Biodiscovery and the Auckland Cancer Society.

REFERENCES

1 Shepherd, P. R., Withers, D. J. and Siddle, K. (1998) Phosphoinositide 3-kinase: the key switch mechanism in insulin signalling. Biochem. J. **333**, 471–490
2 Liu, P., Cheng, H., Roberts, T. M. and Zhao, J. J. (2009) Targeting the phosphoinositide 3-kinase pathway in cancer. Nat. Rev. Drug Discov. **8**, 627–644
3 Vanhaesebroeck, B., Guillermet-Guibert, J., Graupera, M. and Bilanges, B. (2010) The emerging mechanisms of isoform-specific PI3K signalling. Nat. Rev. Mol. Cell Biol. **11**, 329–341
4 Navé, B. T., Haigh, R. J., Hayward, A. C., Siddle, K. and Shepherd, P. R. (1996) Compartment specific regulation of phosphoinositide 3-kinase by PDGF and insulin in 3T3-L1 adipocytes. Biochem. J. **318**, 55–60
5 Navé, B. T., Siddle, K. and Shepherd, P. R. (1996) Phorbol ester stimulates phosphatidylinositol 3,4,5 tris phosphate production in 3T3-L1 adipocytes: implications for signalling to glucose transport. Biochem. J. **318**, 203–205
6 Beeton, C. A., Chance, E. M., Foukas, L. C. and Shepherd, P. R. (2000) Comparison of the kinetic properties of the lipid and protein kinase activities of the p110α and p110β catalytic subunits of class Ia PI 3-kinases. Biochem. J. **350**, 353–359
7 Leslie, N. R. and Downes, C. P. (2004) PTEN function: how normal cells control it and tumour cells lose it. Biochem. J. **382**, 1–11
8 Chalhoub, N. and Baker, S. J. (2009) PTEN and the PI3-kinase pathway in cancer. Annu. Rev. Pathol. **4**, 127–50
9 Samuels, Y., Wang, Z., Bardelli, A., Silliman, N., Ptak, J., Szabo, S., Yan, H., Gazdar, A., Powell, S. M., Riggins, G. J. et al. (2004) High frequency of mutations of the PIK3CA gene in human cancers. Science **304**, 554
10 Campbell, I. G., Russell, S. E., Choong, D. Y. H., Montgomery, K. G., Ciavarella, M. L., Hooi, C. S. F., Cristiano, B. E., Pearson, R. B. and Phillips, W. A. (2004) Mutation of the PIK3CA gene in ovarian and breast cancer. Cancer Res. **64**, 7678–7681
11 Shayesteh, L., Lu, Y., Kuo, W., Baldocchi, R., Godfrey, T., Collins, C., Pinkel, D., Powell, B., Mills, G. B. and Gray, J. W. (1999) PI3KCA is implicated as an oncogene in ovarian cancer. Nat. Genet. **21**, 99–102
12 Carson, J. D., Van Aller, G., Lehr, R., Sinnamon, R. H., Kirkpatrick, R. B., Auger, K. R., Dhanak, D., Copeland, R. A., Gontarek, R. R., Tummino, P. J. and Luo, L. (2008) Effects of oncogenic p110α subunit mutations on the lipid kinase activity of phosphoinositide 3-kinase. Biochem. J. **409**, 519–524
13 Chaussade, C., Cho, K., Mawson, C., Rewcastle, G. W. and Shepherd, P. R. (2009) Functional differences between two classes of oncogenic mutation in the PIK3CA gene. Biochem. Biophys. Res. Commun. **381**, 577–581
14 Bader, A. G., Kang, S. and Vogt, P. K. (2006) Cancer-specific mutations in PIK3CA are oncogenic *in vivo*. Proc. Natl. Acad. Sci. U.S.A. **103**, 1475–1479
15 Isakoff, S. J., Engelman, J. A., Irie, H. Y., Luo, J., Brachmann, S. M., Pearline, R. V., Cantley, L. C. and Brugge, J. S. (2005) Breast cancer-associated PIK3CA mutations are oncogenic in mammary epithelial cells. Cancer Res. **65**, 10992–11000
16 Samuels, Y., Diaz, L. A., Schmidt-Kittler, O., Cummins, J. M., DeLong, L., Cheong, I., Rago, C., Huso, D. L., Lengauer, C., Kinzler, K. W. et al. (2005) Mutant PIK3CA promotes cell growth and invasion of human cancer cells. Cancer Cell **7**, 561–573
17 Engelman, J. A., Chen, L., Tan, X., Crosby, K., Guimaraes, A. R., Upadhyay, R., Maira, M., McNamara, K., Perera, S. A., Song, Y. et al. (2008) Effective use of PI3K and MEK inhibitors to treat mutant Kras G12D and PIK3CA H1047R murine lung cancers. Nat. Med. **14**, 1351–1356
18 Adams, J. R., Xu, K., Liu, J. C., Ruiz Agamez, N. M., Loch, A. J., Wong, R. G., Wang, W., Wright, K. L., Lane, T. F., Zacksenhaus, E. and Egan, S. E. (2011) Cooperation between Pik3ca and p53 mutations in mouse mammary tumor formation. Cancer Res. **71**, 2706–2717
19 Mandelker, D., Gabelli, S. B., Schmidt-Kittler, O., Zhu, J., Cheong, I., Huang, C. H., Kinzler, K. W., Vogelstein, B. and Amzel, L. M. (2009) A frequent kinase domain mutation that changes the interaction between PI3Kα and the membrane. Proc. Natl. Acad. Sci. U.S.A. **106**, 16996–17001
20 Miled, N., Yan, Y., Hon, W. C., Perisic, O., Zvelebil, M., Inbar, Y., Schneidman-Duhovny, D., Wolfson, H. J., Backer, J. M. and Williams, R. L. (2007) Mechanism of two classes of cancer mutations in the phosphoinositide 3-kinase catalytic subunit. Science **317**, 239–242
21 Pang, H., Flinn, R., Patsialou, A., Wyckoff, J., Roussos, E. T., Wu, H., Pozzuto, M., Goswami, S., Condeelis, J. S., Bresnick, A. R. et al. (2009) Differential enhancement of breast cancer cell motility and metastasis by helical and kinase domain mutations of class IA phosphoinositide 3-kinase. Cancer Res. **69**, 8868–8876
22 Vasudevan, K. M., Barbie, D. A., Davies, M. A., Rabinovsky, R., McNear, C. J., Kim, J. J., Hennessy, B. T., Tseng, H., Pochanard, P., Kim, S. Y. et al. (2009) AKT-independent signaling downstream of oncogenic PIK3CA mutations in human cancer. Cancer Cell **16**, 21–32
23 Zhao, L. and Vogt, P. K. (2010) Hot-spot mutations in p110α of phosphatidylinositol 3-kinase (pI3K): differential interactions with the regulatory subunit p85 and with RAS. Cell Cycle **9**, 596–600
24 Marone, R., Cmiljanovic, V., Giese, B. and Wymann, M. P. (2008) Targeting phosphoinositide 3-kinase: moving towards therapy. Biochim. Biophys. Acta **1784**, 159–185
25 Workman, P., Clarke, P. A., Raynaud, F. I. and van Montfort, R. L. (2010) Drugging the PI3 kinome: from chemical tools to drugs in the clinic. Cancer Res. **70**, 2146–2157
26 Wee, S., Wiederschain, D., Maira, S. M., Loo, A., Miller, C., deBeaumont, R., Stegmeier, F., Yao, Y. M. and Lengauer, C. (2008) PTEN-deficient cancers depend on PIK3CB. Proc. Natl. Acad. Sci. U.S.A. **105**, 13057–13062
27 Crowder, R. J., Phommaly, C., Tao, Y., Hoog, J., Luo, J., Perou, C. M., Parker, J. S., Miller, M. A., Huntsman, D. G., Lin, L. et al. (2009) PIK3CA and PIK3CB inhibition produce synthetic lethality when combined with estrogen deprivation in estrogen receptor-positive breast cancer. Cancer Res. **69**, 3955–62
28 Guerreiro, A. S., Fattet, S., Fischer, B., Shalaby, T., Jackson, S. P., Schoenwaelder, S. M., Grotzer, M. A., Delattre, O. and Arcaro, A. (2008) Targeting the PI3K p110α isoform inhibits medulloblastoma proliferation, chemoresistance, and migration. Clin. Cancer Res. **14**, 6761–9
29 Haya kawa, M., Kawaguchi, K., Kaizawa, H., Koizumi, T., Ohishi, T., Yamano, M., Okada, M., Ohta, M., Tsukamoto, S., Raynaud, F. I. et al. (2007) Synthesis and biological evaluation of sulfonylhydrazone-substituted imidazo[1,2-a]pyridines as novel PI3 kinase p110a inhibitors. Bioorg. Med. Chem. **15**, 5837–5844
30 Knight, Z. A., Gonzalez, B., Feldman, M. E., Zunder, E. R., Goldenberg, D. D., Williams, O., Loewith, R., Stokoe, D., Balla, A., Toth, B. et al. (2006) A pharmacological map of the PI3-K family defines a role for p110a in insulin signalling. Cell **125**, 1–15
31 Chaussade, C., Rewcastle, G.W., Kendall, J. D., Denny, W. A., Cho, K., Gronning, L. M., Chong, M. L., Anagnostou, S. H., Jackson, S. P., Daniele, N. and Shepherd, P. R. (2007) Evidence for functional redundancy of class IA PI3K isoforms in insulin signalling. Biochem. J. **404**, 449–458
32 Torbett, N. E., Luna-Moran, A., Knight, Z. A., Houk, A., Moasser, M., Weiss, W., Shokat, K. M. and Stokoe, D. (2008) A chemical screen in diverse breast cancer cell lines reveals genetic enhancers and suppressors of sensitivity to PI3K isoform-selective inhibition. Biochem. J. **415**, 97–110
33 Schmidt-Kittler, O., Zhu, J., Yang, J., Liu, G., Hendricks, W., Lengauer, C., Gabelli, S. B., Kinzler, K. W., Vogelstein, B., Huso, D. L. and Zhou, S. (2010) PI3Kα inhibitors that inhibit metastasis. Oncotarget **1**, 339–348

34 Sun, M., Hillmann, P., Hofmann, B. T., Hart, J. R. and Vogt, P. K. (2010) Cancer-derived mutations in the regulatory subunit p85α of phosphoinositide 3-kinase function through the catalytic subunit p110 α. Proc. Natl. Acad. Sci. U.S.A. **107**, 15547–15552
35 Fairhurst, R. A. and Imbrich, P. (2009) Preparation of N1-bithiazolyl pyrrolidinedicarboxamides and related compounds as phosphatidylinositol 3-kinase inhibitors. PCT Int. Appl., WO 2009/080705
36 Chen, V. B., Arendall, 3rd, W. B., Headd, J. J., Keedy, D. A., Immormino, R. M., Kapral, G. J., Murray, L. W., Richardson, J. S. and Richardson, D. C. (2010) MolProbity: all-atom structure validation for macromolecular crystallography. Acta Crystallogr. Sect. D Biol. Crystallogr. **66**, 12–21
37 Falasca, M., Hughes, W. E., Dominguez, V., Sala, G., Fostira, F., Fang, M. Q., Cazzolli, R., Shepherd, P. R., James, D. E. and Maffucci, T. (2007) The role of phosphoinositide 3-kinase C2α in insulin signaling. J. Biol. Chem. **282**, 28226–28236
38 Backer, J. M. (2008) The regulation and function of Class III PI3Ks: novel roles for Vps34. Biochem. J. **410**, 1–17
39 Minogue, S., Waugh, M. G., De Matteis, M. A., Stephens, D. J., Berditchevski, F. and Hsuan, J. J. (2006) Phosphatidylinositol 4-kinase is required for endosomal trafficking and degradation of the EGF receptor. J. Cell Sci. **119**, 571–580
40 Jackson, S. P., Schoenwaelder, S. M., Goncalves, I., Nesbitt, W. S., Yap, C. L., Wright, C. E., Kenche, V., Anderson, K. E., Dopheide, S. M., Yuan, Y. et al. (2005) PI 3-kinase p110β: a new target for antithrombotic therapy. Nat. Med. **11**, 507–514
41 Balla, A., Tuymetova, G., Toth, B., Szentpetery, Z., Zhao, X., Knight, Z. A., Shokat, K., Steinbach, P. J. and Balla, T. (2008) Design of drug-resistant alleles of type-III phosphatidylinositol 4-kinases using mutagenesis and molecular modeling. Biochemistry **47**, 1599–1607
42 Huang, C. H., Mandelker, D., Schmidt-Kittler, O., Samuels, Y., Velculescu, V. E., Kinzler, K. W., Vogelstein, B., Gabelli, S. B. and Amzel, L. M. (2007) The structure of a human p110α/p85α complex elucidates the effects of oncogenic PI3Kα mutations. Science **318**, 1744–1748
43 Frazzetto, M., Suphioglu, C., Zhu, J., Schmidt-Kittler, O., Jennings, I. G., Cranmer, S. L., Jackson, S. P., Kinzler, K. W., Vogelstein, B. and Thompson, P. E. (2008) Dissecting isoform selectivity of PI3K inhibitors: the role of non-conserved residues in the catalytic pocket. Biochem. J. **414**, 383–390
44 Sabbah, D. A., Vennerstrom, J. L. and Zhong, H. (2010) Docking studies on isoform-specific inhibition of phosphoinositide-3-kinases. J. Chem. Inf. Model. **50**, 1887–1898
45 Baguley, B. C., Marshall, E. S. and Finlay, G. J. (1999) Short-term cultures of clinical tumor material: potential contributions to oncology research. Oncol. Res. **11**, 115–124
46 Kang, S., Denley, A., Vanhaesebroeck, B. and Vogt, P. K. (2006) Oncogenic transformation induced by the p110β, -γ, and -δ isoforms of class I phosphoinositide 3-kinase. Proc. Natl. Acad. Sci. U.S.A. **103**, 1289–1294
47 Chen, H., Mei, L., Zhou, L., Shen, X., Guo, C., Zheng, Y., Zhu, H., Zhu, Y. and Huang, L. (2010) PTEN restoration and PIK3CB knockdown synergistically suppress glioblastoma growth *in vitro* and in xenografts. J. Neuro-oncol., doi:10.1007/s11060-010-0492-2
48 Jia, S., Liu, Z., Zhang, S., Liu, P., Zhang, L., Lee, S. H., Zhang, J., Signoretti, S., Loda, M., Roberts, T. M. and Zhao, J. J. (2008) Essential roles of PI(3)K-p110β in cell growth, metabolism and tumorigenesis. Nature **454**, 776–779
49 Ciraolo, E., Iezzi, M., Marone, R., Marengo, S., Curcio, C., Costa, C., Azzolino, O., Gonella, C., Rubinetto, C., Wu, H. et al. (2008) Phosphoinositide 3-kinase p110β activity: key role in metabolism and mammary gland cancer but not development. Sci. Signaling **1**, ra3
50 Edgar, K. A., Wallin, J. J., Berry, M., Lee, L. B., Prior, W. W., Sampath, D., Friedman, L. S. and Belvin, M. (2010) Isoform-specific phosphoinositide 3-kinase inhibitors exert distinct effects in solid tumors. Cancer Res. **70**, 1164–1172
51 Foukas, L. C., Berenjeno, I. M., Gray, A., Khwaja, A. and Vanhaesebroeck, B. (2010) Activity of any class IA PI3K isoform can sustain cell proliferation and survival. Proc. Natl. Acad. Sci. U.S.A. **107**, 11381–11386
52 Papakonstanti, E. A., Zwaenepoel, O., Bilancio, A., Burns, E., Nock, G. E., Houseman, B., Shokat, K., Ridley, A. J. and Vanhaesebroeck, B. (2008) Distinct roles of class IA PI3K isoforms in primary and immortalised macrophages. J. Cell Sci. **121**, 4124–4133
53 Yuan, T. L., Wulf, G., Burga, L. and Cantley, L. C. (2011) Cell-to-cell variability in PI3K protein level regulates PI3K-AKT pathway activity in cell populations. Curr. Biol. **21**, 173–183
54 Zhao, L. and Vogt, P. (2008) Helical domain and kinase domain mutations in p110α of phosphatidylinositol 3-kinase induce gain of function by different mechanisms. Proc. Natl. Acad. Sci. U.S.A. **105**, 2652–2657
55 Maira, S. M., Stauffer, F., Brueggen, J., Furet, P., Schnell, C., Fritsch, C., Brachmann, S., Chene, P., De Pover, A., Schoemaker, K. et al. (2008) Identification and characterization of NVP-BEZ235, a new orally available dual phosphatidylinositol 3-kinase/mammalian target of rapamycin inhibitor with potent *in vivo* antitumor activity. Mol. Cancer Ther. **7**, 1851–1863

Received 17 March 2011/27 May 2011; accepted 14 June 2011
Published as BJ Immediate Publication 14 June 2011, doi:10.1042/BJ20110502

Biochem. J. (2011) **438**, 53–62 (Printed in Great Britain) doi:10.1042/BJ20110502

online data

SUPPLEMENTARY ONLINE DATA

A drug targeting only p110α can block phosphoinositide 3-kinase signalling and tumour growth in certain cell types

Stephen JAMIESON*†, Jack U. FLANAGAN*†, Sharada KOLEKAR‡, Christina BUCHANAN†‡, Jackie D. KENDALL*†, Woo-Jeong LEE‡, Gordon W. REWCASTLE*†, William A. DENNY*†, Ripudaman SINGH*, James DICKSON§, Bruce C. BAGULEY*† and Peter R. SHEPHERD†‡[1]

*Auckland Cancer Society Research Centre, Faculty of Medical and Health Sciences, University of Auckland, Private Bag 92019, Auckland 1042, New Zealand, †Maurice Wilkins Centre for Molecular Biodiscovery, University of Auckland, Private Bag 92019, Auckland, New Zealand, ‡Department of Molecular Medicine and Pathology, University of Auckland, Medical School, Private Bag 92019, Auckland 1042, New Zealand, and §School of Biological Science, University of Auckland, Private Bag 92019, Auckland 1042, New Zealand

	% Activity remaining A66 10 μM	PIK75 10 μM	TGX221 10 μM	IC87114 10 μM
MKK1	108	4	84	86
MKK2	116	9	114	105
MKK6	85	55	83	97
ERK1	99	16	103	100
ERK2	92	42	103	105
JNK1	90	19	102	95
JNK2	102	62	86	90
JNK3	106	56	104	101
p38a MAPK	96	98	92	93
p38b MAPK	98	62	99	94
p38g MAPK	90	4	78	100
p38d MAPK	95	2	74	93
ERK8	91	18	102	98
RSK1	84	3	88	99
RSK2	99	4	84	113
PDK1	94	22	99	100
PKBa	97	4	122	103
PKBb	99	70	79	105
SGK1	88	22	103	108
S6K1	98	3	101	104
PKA	89	4	93	94
ROCK 2	100	2	105	97
PRK2	90	1	82	80
PKCa	90	15	103	98
PKCz	110	39	102	106
PKD1	92	36	93	105
MSK1	115	11	90	93
MNK1	91	87	99	94
MNK2	102	47	99	96
MAPKAP-K	105	19	98	98
MAPKAP-K	90	96	83	106
PRAK	85	24	97	98
CAMKKb	93	24	102	116
CAMK1	109	61	92	98
SmMLCK	81	8	98	94
PHK	98	4	87	94

	% Activity remaining A66 10 μM	PIK75 10 μM	TGX221 10 μM	IC87114 10 μM
DAPK1	81	2	102	110
CHK1	97	76	100	146
CHK2	117	34	105	88
GSK3b	95	1	28	98
CDK2-Cyclin	103	2	81	90
PLK1	112	13	89	92
Aurora A	112	13	102	103
Aurora B	109	38	96	98
LKB1	105	10	85	89
AMPK	108	16	98	108
MARK1	97	5	94	96
MARK2	86	36	105	86
MARK3	83	2	99	98
MARK4	87	43	100	103
BRSK1	106	70	185	97
BRSK2	92	30	78	106
MELK	116	4	96	102
NUAK1	81	22	77	100
CK1	95	6	86	90
CK2	91	4	82	111
DYRK1A	96	0	83	94
DYRK2	86	5	89	87
DYRK3	83	-1	85	97
NEK2a	111	9	94	98
NEK6	89	112	95	111
IKKb	114	46	91	95
IKKe	68	8	86	95
TBK1	83	54	93	97
PIM1	111	8	76	102
PIM2	102	13	87	91
PIM3	97	12	64	81
SRPK1	95	83	98	117
EF2K	94	86	92	65
HIPK1	88	8	109	89
HIPK2	100	4	78	98
HIPK3	92	10	99	97
CLK2	20	1	41	89
PAK2	85	14	102	100

	% Activity remaining A66 10 μM	PIK75 10 μM	TGX221 10 μM	IC87114 10 μM
PAK4	100	8	89	71
PAK5	85	29	86	85
PAK6	93	33	105	91
MST2	94	14	101	120
MST4	99	16	103	100
GCK	71	22	121	103
MINK1	100	6	101	106
MEKK1	135	13	92	97
MLK1	83	26	99	100
MLK3	99	13	104	93
TAO1	97	8	73	90
ASK1	93	12	94	94
TAK1	105	6	88	103
IRAK4	67	23	107	105
RIPK2	22	19	76	113
TTK	84	15	74	92
Src	115	19	84	95
Lck	111	6	61	96
CSK	108	22	88	92
YES1	113	19	58	88
BTK	96	6	67	105
JAK2	95	2	99	88
SYK	118	20	101	88
EPH-A2	126	71	76	111
EPH-A4	114	13	63	107
EPH-B1	106	77	99	108
EPH-B2	87	8	84	101
EPH-B3	114	8	115	108
EPH-B4	95	27	73	94
FGF-R1	116	11	86	93
HER4	108	13	111	108
IGF-1R	90	7	105	104
IR	108	4	97	96
IRR	99	12	85	97
TrkA	103	8	70	91
VEG-FR	97	11	78	93

Figure S1 Activity of kinases after addition of A66, PIK-75, TGX-221 or IC87114

[1] To whom correspondence should be addressed (email peter.shepherd@auckland.ac.nz).

Conflict of interest statement: P.R.S., W.A.D., J.D.K. and G.W.R. have consulted for and own stock in Pathway Therapeutics, a company developing PI3K inhibitors, although none of these compounds are used in the present study.

Enzyme	% Inhibition by 10 μM A66
ABL1	14
ABL1 E255K	11
ABL1 G250E	8
ABL1 T315I	8
ABL1 Y253F	8
ABL2 (Arg)	-3
ACVR1 (ALK2)	47
ACVR1B (ALK4)	-2
ACVR2B	-2
ADRBK1 (GRK2)	-1
ADRBK2 (GRK3)	-4
AKT1 (PKB alpha)	-1
AKT2 (PKB beta)	-9
AKT3 (PKB gamma)	-13
AMPK A1/B1/G1	-1
AMPK A2/B1/G1	-3
AURKA (Aurora A)	-3
AURKB (Aurora B)	2
AURKC (Aurora C)	12
AXL	14
BLK	6
BMPR1A (ALK3)	12
BMX	3
BRAF	-10
BRAF	4
BRAF V599E	-13
BRAF V599E	7
BRSK1 (SAD1)	-4
BTK	-2
CAMK1 (CaMK1)	29
CAMK1D (CaMKI delta)	-3
CAMK2A (CaMKII alpha)	-2
CAMK2B (CaMKII beta)	-4
CAMK2D (CaMKII delta)	-3
CAMK4 (CaMKIV)	-8
CAMKK1 (CAMKKA)	2
CAMKK2 (CaMKK beta)	14
CDC42 BPA (MRCKA)	-14
CDC42 BPB (MRCKB)	7
CDK1/cyclin B	-1
CDK2/cyclin A	3
CDK5/p25	1
CDK5/p35	-1
CDK7/cyclin H/MNAT1	-20
CDK8/cyclin C	13
CDK9/cyclin K	-1
CDK9/cyclin T1	-16
CHEK1 (CHK1)	19
CHEK2 (CHK2)	-3
CHUK (IKK alpha)	11
CLK1	27
CLK2	58
CLK3	28
CLK4	87
CSF1R (FMS)	9
CSK	7
CSNK1A1 (CK1 alpha 1)	0
CSNK1D (CK1 delta)	3
CSNK1E (CK1 epsilon)	7
CSNK1G1 (CK1 gamma 1)	-5
CSNK1G2 (CK1 gamma 2)	10
CSNK1G3 (CK1 gamma 3)	3
CSNK2A1 (CK2 alpha 1)	7
CSNK2A2 (CK2 alpha 2)	1
DAPK1	-37
DAPK3 (ZIPK)	0
DCAMKL2 (DCK2)	0
DDR1	3
DDR2	2
DMPK	1
DNA-PK	12
DYRK1A	14
DYRK1B	4
DYRK3	-12
DYRK4	-2
EEF2K	-5
EGFR (ErbB1)	0
EGFR (ErbB1) L858R	-3
EGFR (ErbB1) L861Q	-1
EGFR (ErbB1) T790M	7
EGFR (ErbB1) T790M L858R	6
EPHA1	-1
EPHA2	-3
EPHA3	16
EPHA4	19
EPHA5	2
EPHA7	-2
EPHA8	-3
EPHB1	2
EPHB2	4
EPHB3	0
EPHB4	-9
ERBB2 (HER2)	4
ERBB4 (HER4)	-10
FER	-10
FES (FPS)	0
FGFR1	1
FGFR2	9
FGFR3	18
FGFR3 K650E	11

Enzyme	% Inhibition by 10 μM A66
FGFR4	16
FGR	6
FLT1 (VEGFR1)	0
FLT3	12
FLT3 D835Y	4
FLT4 (VEGFR3)	14
FRAP1 (mTOR)	2
FRK (PTK5)	2
FYN	6
GRK4	-8
GRK5	0
GRK6	8
GRK7	4
GSG2 (Haspin)	-14
GSK3A (GSK3 alpha)	-6
GSK3B (GSK3 beta)	-1
HCK	3
HIPK1 (Myak)	-12
HIPK2	4
HIPK3 (YAK1)	-2
HIPK4	30
IGF1R	-9
IKBKB (IKK beta)	-1
IKBKE (IKK epsilon)	0
INSR	1
INSRR (IRR)	1
IRAK1	-18
IRAK4	6
ITK	-7
JAK1	10
JAK2	19
JAK2 JH1 JH2	15
JAK2 JH1 JH2 V617F	3
JAK3	14
KDR (VEGFR2)	1
KIT	29
KIT T670I	0
KIT V654A	8
LCK	2
LIMK1	7
LIMK2	4
LRRK2	35
LRRK2 G2019S	56
LTK (TYK1)	17
LYN A	0
LYN B	-4
MAP2K1 (MEK1)	-3
MAP2K1 (MEK1)	14
MAP2K1 (MEK1) S218D S222D	5
MAP2K2 (MEK2)	-6
MAP2K2 (MEK2)	10
MAP2K3 (MEK3)	-7
MAP2K6 (MKK6)	-10
MAP2K6 (MKK6)	8
MAP2K6 (MKK6) S207E T211E	-7
MAP3K10 (MLK2)	10
MAP3K11 (MLK3)	5
MAP3K14 (NIK)	0
MAP3K2 (MEKK2)	-19
MAP3K3 (MEKK3)	10
MAP3K5 (ASK1)	-5
MAP3K7/MAP3K7IP1 (TAK1-TAB1	15
MAP3K8 (COT)	-17
MAP3K9 (MLK1)	32
MAP4K2 (GCK)	8
MAP4K4 (HGK)	11
MAP4K5 (KHS1)	10
MAPK1 (ERK2)	-2
MAPK10 (JNK3)	-5
MAPK10 (JNK3)	29
MAPK11 (p38 beta)	8
MAPK12 (p38 gamma)	-5
MAPK13 (p38 delta)	-7
MAPK14 (p38 alpha)	15
MAPK14 (p38 alpha) Direct	4
MAPK3 (ERK1)	-10
MAPK8 (JNK1)	14
MAPK8 (JNK1)	6
MAPK9 (JNK2)	6
MAPK9 (JNK2)	18
MAPKAPK2	2
MAPKAPK3	4
MAPKAPK5 (PRAK)	-6
MARK1 (MARK)	-8
MARK2	-19
MARK3	-5
MARK4	-15
MATK (HYL)	0
MELK	11
MERTK (cMER)	1
MET (cMet)	20
MET M1250T	2
MINK1	-3
MKNK1 (MNK1)	-7
MKNK2 (MNK2)	3
MLCK (MLCK2)	16
MST1R (RON)	9
MST4	2
MUSK	-9
MYLK (MLCK)	2

Enzyme	% Inhibition by 10 μM A66
MYLK2 (skMLCK)	-2
NEK1	18
NEK2	10
NEK4	-3
NEK6	2
NEK7	-6
NEK9	-8
NLK	6
NTRK1 (TRKA)	14
NTRK2 (TRKB)	2
NTRK3 (TRKC)	8
NUAK1 (ARK5)	-18
PAK1	2
PAK2 (PAK65)	-1
PAK3	10
PAK4	0
PAK6	10
PAK7 (KIAA1264)	11
PASK	1
PDGFRA (PDGFR alpha)	8
PDGFRA D842V	11
PDGFRA T674I	3
PDGFRA V561D	4
PDGFRB (PDGFR beta)	-3
PDK1	-1
PDK1 Direct	-1
PHKG1	4
PHKG2	-1
PI4KA (PI4K alpha)	-19
PI4KB (PI4K beta)	98
PIK3C2A (PI3K-C2 alpha)	-2
PIK3C2B (PI3K-C2 beta)	77
PIK3C3 (hVPS34)	21
PIK3CA/PIK3R1 (p110 alpha/p85 alp	96
PIK3CD/PIK3R1 (p110 delta/p85 alp	91
PIK3CG (p110 gamma)	86
PIM1	-4
PIM2	-4
PKN1 (PRK1)	-19
PLK1	-3
PLK2	-24
PLK3	3
PRKACA (PKA)	-2
PRKCA (PKC alpha)	2
PRKCB1 (PKC beta I)	3
PRKCB2 (PKC beta II)	-10
PRKCD (PKC delta)	3
PRKCE (PKC epsilon)	9
PRKCG (PKC gamma)	6
PRKCH (PKC eta)	9
PRKCI (PKC iota)	9
PRKCN (PKD3)	7
PRKCQ (PKC theta)	10
PRKCZ (PKC zeta)	3
PRKD1 (PKC mu)	12
PRKD2 (PKD2)	7
PRKG1	-2
PRKG2 (PKG2)	-5
PRKX	-3
PTK2 (FAK)	4
PTK2B (FAK2)	10
PTK6 (Brk)	4
RAF1 (cRAF) Y340D Y341D	-4
RAF1 (cRAF) Y340D Y341D	14
RET	0
RET V804L	-3
RET Y791F	5
RIPK2	66
ROCK1	2
ROCK2	-17
ROS1	11
RPS6KA1 (RSK1)	-1
RPS6KA2 (RSK3)	-4
RPS6KA3 (RSK2)	1
RPS6KA4 (MSK2)	-10
RPS6KA5 (MSK1)	-6
RPS6KA6 (RSK4)	1
RPS6KB1 (p70S6K)	0
SGK (SGK1)	-3
SGK2	4
SGKL (SGK3)	8
SLK	2
SNF1LK2	-5
SPHK1	10
SPHK2	-23
SRC	11
SRC N1	8
SRMS (Srm)	8
SRPK1	2
SRPK2	0
STK16 (PKL12)	-4
STK17A (DRAK1)	11
STK22B (TSSK2)	-12
STK22D (TSSK1)	-7
STK23 (MSSK1)	2
STK24 (MST3)	-2
STK25 (YSK1)	-1
STK3 (MST2)	12
STK33	-5
STK4 (MST1)	11

Enzyme	% Inhibition by 10 μM A66
SYK	8
TAOK2 (TAO1)	0
TAOK3 (JIK)	3
TBK1	-9
TEC	17
TEK (Tie2)	19
TGFBR1 (ALK5)	-2
TNK2 (ACK)	8
TTK	-10
TXK	1
TYK2	-8
TYRO3 (RSE)	5
WEE1	6
WNK2	10
YES1	9
ZAK	5
ZAP70	4

Legend

< 40% Inhibition

40% - 80% Inhibition

≥ 80% Inhibition

Figure S2 Inhibition of kinases by A66

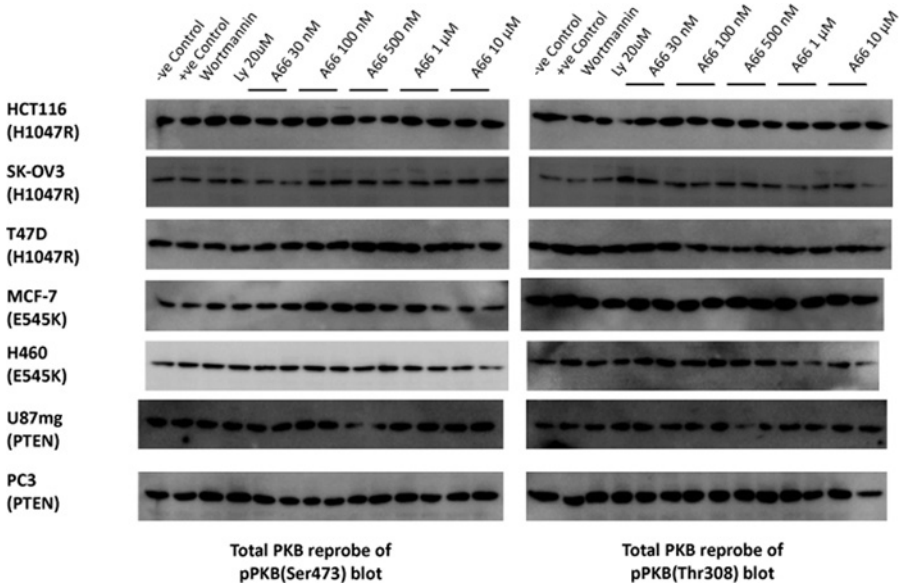

Figure S3 Reprobes of blots in Figure 3 of the main paper with the total PKB antibody

Ly, LY294002.

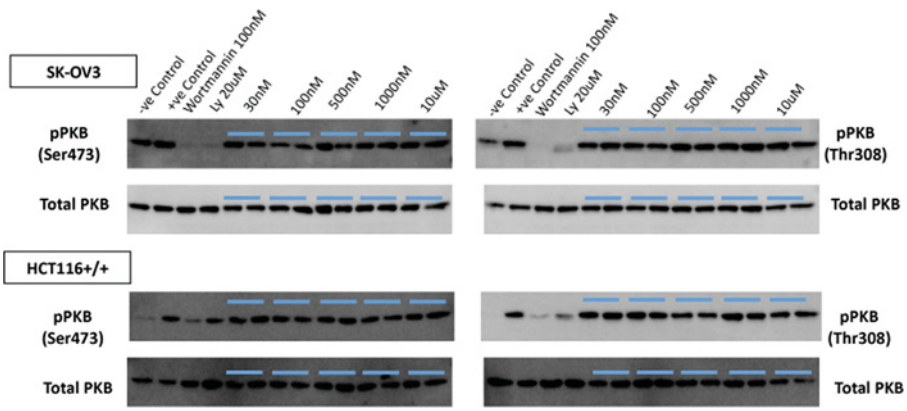

Figure S4 A66 *R* enantiomer does not block signalling to PKB in cells with the *PIK3CA* H1047R mutation

Experiments were performed as in Figure 3 of the main paper, except that the *R* form of A66 was used. Ly, LY294002.

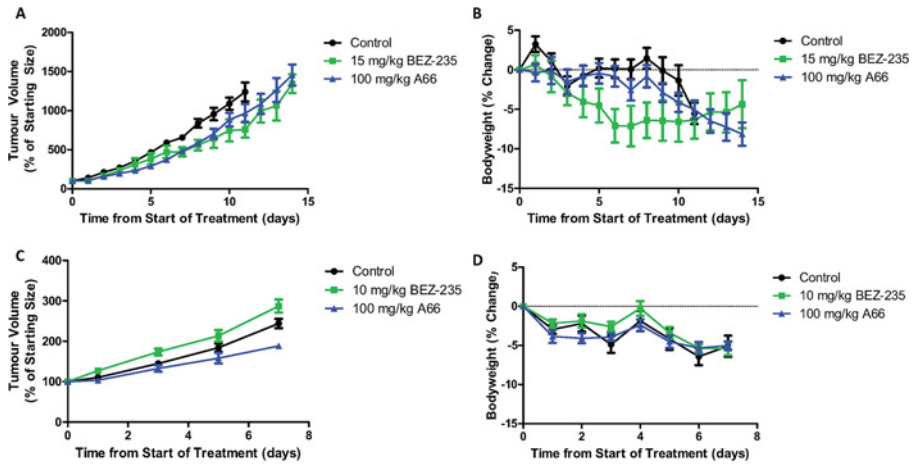

Figure S5 ***In vivo*** **antitumour efficacy and body weight change following treatment with A66 and BEZ-235 in the U87MG and HCT-116 tumour xenograft models**

(**A**) Average tumour volume and (**B**) body weight loss during QD×14 dosing with 100 mg of A66/kg of body weight and 15 mg of BEZ-235/kg of body weight in mice with U87MG tumours. (**C**) Average tumour volume and (**D**) body weight loss during QD×7 dosing with 100 mg of A66/kg of body weight and 10 mg of BEZ-235/kg of body weight in mice with HCT-116 tumours. Bars represent the means ± S.E.M. for five to seven animals.

Received 17 March 2011/27 May 2011; accepted 14 June 2011
Published as BJ Immediate Publication 14 June 2011, doi:10.1042/BJ20110502